

# Two-Photon Fluorescence Lifetime Imaging (2P-FLIM) for Ion Sensing in Living Cells

Carsten Hille, Mattes Lahn, Carsten Dosche, InnoProfile Junior Research Group “Applied Laser Sensing”, University of Potsdam  
 Felix Koberling, PicoQuant GmbH



PICOQUANT



## Introduction

This application note describes the powerful fusion of fluorescence lifetime imaging microscopy with two-photon excitation (2P-FLIM) by using the PicoQuant time-resolved confocal fluorescence microscope MicroTime 200.

The intracellular ion homeostasis in living cells is one requirement for optimal physiological functionality in living systems. One of the most prominent features in living organisms is the intracellular pH ( $pH_i$ ) since it affects many physiological processes such as cellular metabolism, ion channel conductivity, contractility, ion transport and cell cycle control [1]. On the other hand, chloride, together with bicarbonate, is the major physiological anion in living cells and it is involved in the regulation of  $pH_i$ , cell volume, fluid secretion and signalling processes [2]. Thus, the adequate quantitative monitoring of intracellular ion concentrations can improve our knowledge about physiological functions in living systems.

Fluorescence microscopy has become one of the most powerful tools for investigating physiological processes on cellular scales providing higher contrast than classical microscopic methods. Moreover, specific fluorescent dyes offer the unique possibility to detect the distribution of analytes even within single cells. A favourable approach for the detection of fluorescent dyes is to measure their fluorescence decay time by using the fluorescence lifetime imaging microscopy (FLIM) technique. In contrast to the fluorescence intensity, the fluorescence decay time is mostly independent of variations in dye concentration, illumination intensity or processes such as photobleaching and dye leakage [3]. Thus, absolute quantification of ion concentrations in biological preparations by using FLIM for ion-sensitive fluorescent dyes can be more reliable.

Among FLIM, additional improvement can be achieved by two-photon (2P) excitation, which is nowadays a well-established technique in modern biological research [4]. Because of the nonlinear process of 2P excitation the generated fluorescence is restricted only to the small focal volume. As a consequence, there is no necessity of a pinhole before the detector to reject out-of-

focus fluorescence light for confocal detection, increasing the detectable fluorescence signal. Furthermore, most biological tissues strongly scatter visible light making high-resolution deep imaging impossible for classical confocal microscopy. The less-scattered near infrared (NIR) excitation light as used in 2P microscopy can overcome this limitation allowing deep tissue imaging and penetration depths up to 1 mm. In addition, low-energy NIR excitation light and the highly localised excitation strongly reduce global photobleaching of the fluorescent dye as well as tissue damages.

## Experimental 2P-FLIM setup

Intracellular ion measurements in an insect tissue were performed by using the PicoQuant MicroTime 200 confocal fluorescence lifetime microscope system, based on an inverted microscope (IX 71, Olympus) equipped with a 100x/NA 1.4 oil immersion objective (Olympus PlanApo), on which the sample chamber could be mounted (Fig.1) [5].

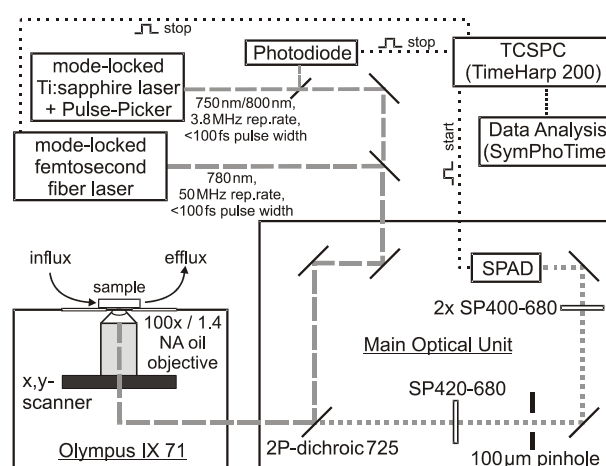


Fig. 1: 2P-FLIM setup, based on the PicoQuant MicroTime 200 fluorescence lifetime microscope system.

2P excitation was realised by a mode-locked Ti:Sapphire laser system (Tsunami & Millennia, Spectra Physics) operating at wavelengths between 750 nm and 800 nm, 80 MHz pulse

repetition rate and ~100 fs pulse width. The pulse repetition rate was reduced to 3.8 MHz by an acousto-optical single pulse selector (Pulse-Select, APE). Mode-locked Ti:Sapphire infrared pulsed lasers have nearly ideal properties for 2P microscopy and are generally favoured. However, it is an expensive system which prevents many researchers from upgrading existing 1P microscopy systems. An inexpensive alternative is a non-tunable laser working at a fixed wavelength. The non-tuneability is not necessarily a disadvantage, because in comparison to 1P absorption spectra, 2P absorption spectra tend to be broader, meaning that a non-tunable laser can excite spectrally different dyes, even simultaneously. Thus, 2P excitation was also performed by a mode-locked femtosecond fiber laser (C-Fiber A 780, MenloSystems) operating at wavelength 780 nm, 50 MHz pulse repetition rate and ~100 fs pulse width.

The NIR laser beam was coupled into the MicroTime 200 Main Optical Unit via the free space laser port and guided towards the objective via the microscope sideport using two dichroic mirrors (2P-dichroic 725, Chroma). The average power of the NIR laser beam could be optionally adjusted by a circular neutral density filter before entering the MicroTime 200. Images were acquired by rasterscanning the objective with a xy-piezopositioner (Physik Instrumente). One drawback of 2P microscopy compared with 1P microscopy is the lower spatial resolution due to longer excitation wavelengths. However, the situation can be improved by still using the confocal pinhole. Thus, the fluorescence was guided through a 100  $\mu\text{m}$  pinhole and three shortpass filters (1 $\times$  SP420-680 Baader, 2 $\times$  SP400-680 Edmund Optics), in order to cut off all excitation light.

The fluorescence light was detected with a single-photon avalanche diode (SPAD, SPCM-AQR-13, Perkin Elmer) and processed by a TimeHarp 200 PC-board (PicoQuant) using time-correlated single photon counting (TCSPC). The photon data was stored in the time-tagged time-resolved (TTTR) mode, recording every detected photon with its individual timing. A small percentage of the laser light from the Ti:Sapphire laser was directed onto a photodiode (TDA 200, PicoQuant) in order to provide a suited synchronisation signal for the timing electronics. When using the fiber laser, a reference signal provided by the fiber laser itself was used for synchronisation. Overview images of 80  $\mu\text{m}$   $\times$  80  $\mu\text{m}$  were acquired in 60 s - 90 s, and detailed sections of around 25  $\mu\text{m}$   $\times$  25  $\mu\text{m}$  were acquired in 30 s and the acquisition time per pixel was varied from 0.6 ms to 2.0 ms. Data acquisition and analysis were performed using the SymPhoTime software (PicoQuant). The quality of fluorescence decay tail-fitting was estimated by small residuals and small  $\chi^2$  values.

## Performance of the 2P-FLIM setup

The instrument response function (IRF) of the entire setup was obtained by detecting the backscattered excitation light from a cover slip surface. Although the pulsed excitation light features a ~100 fs pulse width, the full width at half maximum (FWHM) of the IRF curve was typically 300 ps - 400 ps and is thus mainly determined by the SPAD detector response time.

To test whether the instrumental setup was able to perform 2P fluorescence excitation, measurements on the known 2P excitable fluorescent dye fluorescein [6] were carried out. The typical quadratic dependence of the generated fluorescence  $I$  on the average excitation light power  $P_{\text{av}}$  as given by the following equation

$$I \propto P_{\text{av}}^2 \Leftrightarrow \log(I) \propto 2 \times \log(P_{\text{av}}) ,$$

reveals 2P excitation in a double-logarithmic plot with a slope of nearly 2 [4]. Therefore the total photon counts detected by the SPAD were measured as a function of the average excitation laser power (Fig. 2).

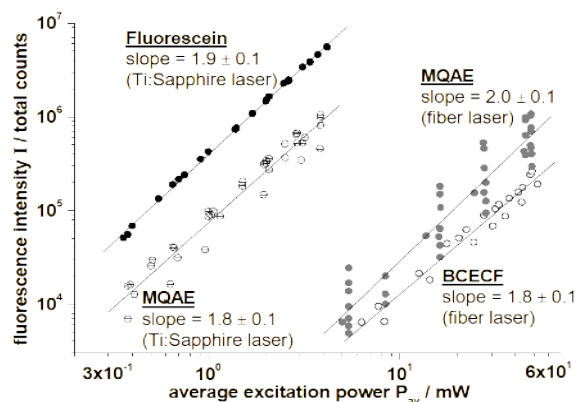


Fig. 2: Fluorescence intensity dependence on the average excitation power to proof the 2P excitation: Double-logarithmic plot for fluorescein in 0.1 M NaOH solution as well as MQAE and BCECF loaded into salivary duct cells.

The fluorescence intensity of fluorescein varied nearly as the square of the average excitation laser power (slope:  $1.9 \pm 0.1$ ), indicating that fluorescein was excited by absorption of two photons of 800 nm wavelength. In order to test the accurate determination of fluorescence decay times by the 2P-FLIM setup, the fluorescence decay times of fluorescein were also measured at two different pH values. From the single-exponential fluorescence decays of 5  $\mu\text{M}$  fluorescein at pH 1 and pH 13 decay times of 3.08 ns  $\pm$  0.01 ns (number of independent measurements:  $N = 17$ ) and 3.99 ns  $\pm$  0.01 ns ( $N = 44$ ) were calculated, respectively. These data correspond well to previously published data for the pH-dependence of the fluorescein decay times [7].

## 2P-FLIM measurements of $[Cl^-]_i$ and $pH_i$ in living tissues

To demonstrate the performance of this 2P-FLIM setup for biological applications the salivary glands of an insect (American cockroach *Periplaneta americana*, a well known model system for studying epithelial ion transport processes), were isolated and loaded with different fluorescent dyes for monitoring the intracellular pH ( $pH_i$ ) and the intracellular chloride concentration ( $[Cl^-]_i$ ). When loaded into the salivary duct cells, the dyes showed a bi-exponential fluorescence decay. However, for an easy calibration and quantification the intensity-weighted average fluorescence decay time  $\tau_{av}$  was calculated by the equation

$$\tau_{av} = (\alpha_1 \times \tau_1^2 + \alpha_2 \times \tau_2^2) / (\alpha_1 \times \tau_1 + \alpha_2 \times \tau_2),$$

where  $\tau_{1/2}$  are the fluorescence decay times and  $\alpha_{1/2}$  are the corresponding amplitudes at  $t = 0$  [8]. To quantify the dependence of  $\tau_{av}$  on  $pH_i$  or  $[Cl^-]_i$  *in situ* calibration experiments were performed.

### $pH_i$ -measurements:

The pH-sensitive fluorescent dye BCECF (2',7'-bis-(2-carboxyethyl)-5-(and-6)-carboxyfluorescein) is by far the most popular fluorescent dye for monitoring  $pH_i$ . Here, BCECF is used for time-resolved fluorescence measurements. BCECF loaded into salivary duct cells exhibited 2P excitation, when excited at 780 nm (fiber laser) as shown in Fig. 2. The bi-exponential fluorescence decay of BCECF corresponded to the deprotonated and protonated species, and their fractions display opposite changes when varying  $pH_i$ . The BCECF average fluorescence decay time  $\tau_{av}$  varied within the physiological  $pH_i$  range from 3.27 ns (pH 6.4) to 3.65 ns (pH 8.4) (Fig. 3A).

Thus, in contrast to *in vitro* calibrations the BCECF  $\tau_{av}$  showed a narrower dynamic range within the

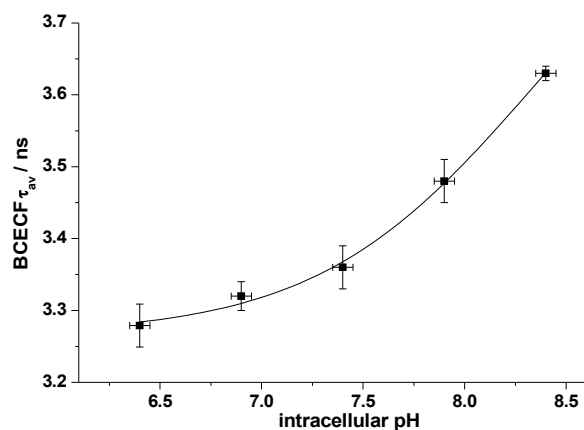


Fig. 3 (A): The pH-dependence of the average fluorescence decay time  $\tau_{av}$  of BCECF loaded into salivary duct cells.

physiological  $pH_i$  region when loaded into living cells.

After successful *in situ* calibration experiments  $pH_i$  was determined in the cockroach salivary duct cells under resting conditions. However, the  $\tau_{av}$  values displayed no striking variations within the duct cells, thus no noticeable  $pH_i$ -microdomains could be observed (Fig. 3B).

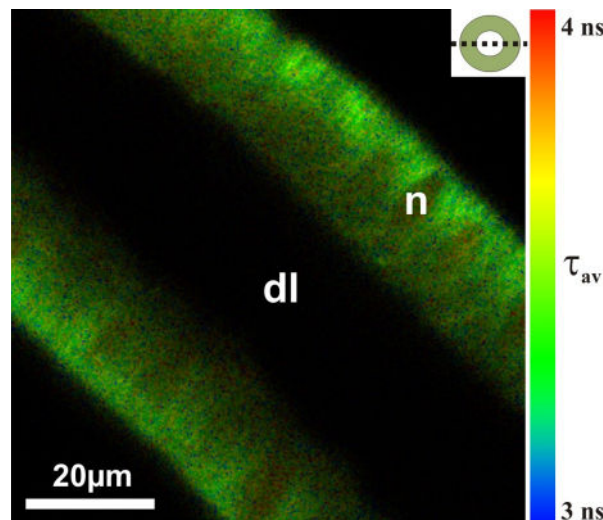


Fig. 3 (B): FLIM-image ( $80 \mu m \times 80 \mu m$ ,  $300 \times 300$  pixel, 0.6 ms acquisition time per pixel) of a BCECF-loaded salivary duct; the optical section plane through the duct is indicated top right; dl = duct lumen; n = nucleus.

By integrating all pixels of an image the mean BCECF  $\tau_{av}$  was calculated to  $3.34 \text{ ns} \pm 0.02 \text{ ns}$  ( $N = 12$ ) corresponding to a  $pH_i$  value of  $pH 7.3 \pm 0.1$  [9]. These values determined with 2P-FLIM are in good agreement with data obtained with invasive pH-sensitive microelectrodes [10].

### $[Cl^-]_i$ -measurements:

The  $Cl^-$ -sensitive fluorescent dye MQAE (N-(ethoxycarbonylmethyl) - 6 - methoxy - quinolinium bromide) was used for time-resolved fluorescence measurements in order to monitor  $[Cl^-]_i$  (Fig. 4). MQAE loaded into salivary duct cells exhibited 2P excitation, when excited at 750 nm (Ti:Sapphire laser) or at 780 nm (fiber laser) as shown in Fig. 2. The MQAE fluorescence decay time is reduced by  $Cl^-$  through dynamic quenching. Thus, the  $[Cl^-]_i$  dependence of  $\tau_{av}$  is described by the Stern-Volmer equation

$$\tau_{av(0)} / \tau_{av} = 1 + K_{SV} \times [Cl^-]_i,$$

where  $\tau_{av(0)}$  is the average fluorescence decay time in the absence of chloride and  $K_{SV}$  is the Stern-Volmer quenching constant and indicates the  $Cl^-$ -sensitivity of MQAE [8]. By exposing the salivary ducts to the calibration solutions, MQAE  $\tau_{av}$  decreased from  $\sim 5.9 \text{ ns}$  to  $\sim 3.4 \text{ ns}$  when increasing  $[Cl^-]_i$  from 0 mM to 75 mM. The Stern-Volmer plot

revealed a quenching constant  $K_{SV} = 9.6 \text{ M}^{-1}$ , which is quite similar to values determined previously in other cell types [e.g. 11].

To determine  $[\text{Cl}^-]_i$  under resting conditions the salivary ducts were first scanned at low resolution in order to get an overview image and after that regions of interest could be scanned again at higher resolution. The fluorescence intensity image showed that MQAE fluorescence was not homogeneously distributed within the duct cells

(as observed for BCECF-loaded duct cells).

In fact, the nuclei were weaker stained and the cytosol seemed to be stained in a lamellar manner. This could be due to the fact that the duct cells have deep infoldings of the basolateral membrane which, in addition, contain many mitochondria. The FLIM-images displayed no clear  $[\text{Cl}^-]_i$  micro-domains and the mean MQAE  $\tau_{av}$  was calculated to  $3.69 \text{ ns} \pm 0.02 \text{ ns}$  ( $N = 48$ ) corresponding to a  $[\text{Cl}^-]_i$  value of  $59 \text{ mM} \pm 1 \text{ mM}$  [12].

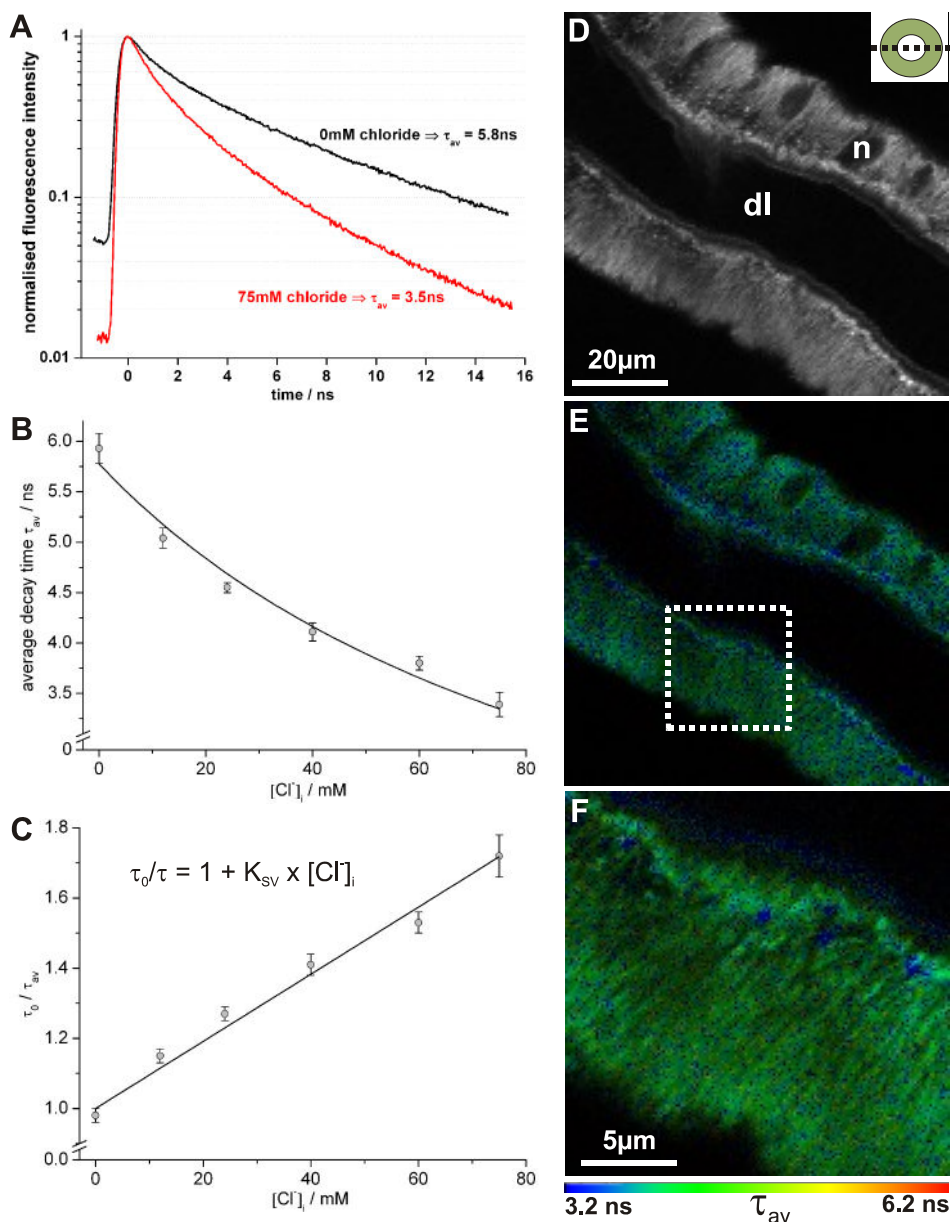


Fig. 4:

- (A) Bi-exponential fluorescence decay curves of MQAE loaded into salivary ducts at two different chloride concentrations.
- (B) Dependence of the MQAE average fluorescence decay time  $\tau_{av}$  on the intracellular chloride concentration  $[\text{Cl}^-]_i$ .
- (C) Stern-Volmer plot of the data shown in B revealing the Stern-Volmer quenching constant  $K_{SV}$  from the slope.
- (D) Fluorescence intensity image of a MQAE loaded salivary duct ( $80 \times 80 \mu\text{m}$ ,  $150 \times 150$  pixel, 2.0 ms acquisition time per pixel); the optical section plane through the duct is indicated top right; dl = duct lumen; n = nucleus).
- (E) FLIM-image of the duct shown in E.
- (F) Enlarged FLIM-image ( $25 \times 25 \mu\text{m}$ ,  $150 \times 150$  pixel, 2.0 ms acquisition time per pixel) indicated by the white dashed rectangle in E.

## Conclusions

This study described the feasibility of fluorescence lifetime imaging microscopy in combination with two-photon excitation (2P-FLIM) for investigating intracellular ion concentrations in living biological tissues. The method is based on lifetime-sensitive dyes acting as local sensors to quantify spatially resolved  $\text{pH}_i$  and  $[\text{Cl}^-]$ . We presented a straight forward *in situ* calibration method to link the fluorescence decay properties with the respective ion concentration and present spatially resolved ion concentration measurements under resting condition in living tissue in living tissue. The  $\text{Cl}^-$ -sensitive dye

MQAE proves to be well suited to map chloride concentrations in the physiologically relevant range, whereas the pH-sensitive dye BCECF still offers only a limited dynamic range regarding fluorescence decay time changes under physiologically pH values. Nevertheless, this technique with the advantages of reliable concentration quantification and reduced dye and tissue damage can be also applied for other biological systems. More details about these measurements can also be found in the final publications [9, 12].

## Acknowledgement

This work was funded by the German Federal Department for Science and Education BMBF.



## References

- [1] Madshus, I.H., Biochem J , 250:1-8 (1988)
- [2] Jentsch T.J., Stein V., Weinreich F., Zdebik A.A., Physiol Rev., 82:503-568 (2002)
- [3] Suhling K., French P.M.W., Phillips D., Photochem Photobiol Sci., 4:13-22 (2005)
- [4] Zipfel W.R., Williams R.M., Webb W.W., Nature Biotechnol, 21:1369-1377(2003)
- [5] Visit product page of MicroTime 200 on picoquant.com
- [6] Xu C., Zipfel W., Shear J.B., et al., Proc Natl Acad Sci, 93:10763-10768 (1996)
- [7] Sjöback R., Nygren J., Kubista M., Spectrochim Acta A, 51:L7-L21 (1995)
- [8] Lakowicz J.R., Principles of fluorescence spectroscopy. 3<sup>rd</sup> ed, Springer (2007)
- [9] Hille C., Berg M., Bressel L., et al. Anal Bional Chem, 391:1871-1879 (2008)
- [10] Hille C., Walz B., J Exp Biol, 210:1463-1471 (2007)
- [11] Lau K.R., Evans R.L., Case R.M., Pflügers Arch, 427:24-32 (1994)
- [12] Hille C., Lahn M., Löhmannsröben H.G., Dosche C. Photochem Photobiol Sci (submitted)

---

Copyright of this document belongs to PicoQuant GmbH. No parts of it may be reproduced, translated or transferred to third parties without written permission of PicoQuant GmbH. All Information given here is reliable to our best knowledge. However, no responsibility is assumed for possible inaccuracies or omissions. Specifications and external appearances are subject to change without notice.

---



PicoQuant GmbH  
Rudower Chaussee 29 (IGZ)  
D-12489 Berlin  
Germany

Phone +49-30-1208820-89  
Email [info@picoquant.com](mailto:info@picoquant.com)  
WWW [www.picoquant.com](http://www.picoquant.com)